PROBABILISTIC ASSESSMENT OF RADIATION RISK FOR SOLAR PARTICLE EVENTS

Myung-Hee Y. Kim[(1)] and Francis A. Cucinotta[(2)]

[(1)] Universities Space Research Association, Houston, TX 77058, myung-hee.y.kim@nasa.gov
[(2)] NASA Johnson Space Center, Houston, TX 77058, francis.a.cucinotta@nasa.gov

ABSTRACT

For long duration missions outside of the protection of the Earth's magnetic field, exposure to solar particle events (SPEs) is a major safety concern for crew members during extra-vehicular activities (EVAs) on the lunar surface or Earth-to-moon or Earth-to-Mars transit. The large majority (~90%) of SPEs have small or no health consequences because the doses are low and the particles do not penetrate to organ depths. However, there is an operational challenge to respond to events of unknown size and duration. We have developed a probabilistic approach to SPE risk assessment in support of mission design and operational planning. Using the historical database of proton measurements during the past 5 solar cycles, the functional form of hazard function of SPE occurrence per cycle was found for non-homogeneous Poisson model. A typical hazard function was defined as a function of time within a non-specific future solar cycle of 4000 days' duration. Distributions of particle fluences for a specified mission period were simulated ranging from its 5^{th} to 95^{th} percentile. Organ doses from large SPEs were assessed using NASA's Baryon transport model, BRYNTRN. The SPE risk was analyzed with the organ dose distribution for the given particle fluences during a mission period. In addition to the total particle fluences of SPEs, the detailed energy spectra of protons, especially at high energy levels, were recognized as extremely important for assessing the cancer risk associated with energetic particles for large events. The probability of exceeding the NASA 30-day limit of blood forming organ (BFO) dose inside a typical spacecraft was calculated for various SPE sizes. This probabilistic approach to SPE protection will be combined with a probabilistic approach to the radiobiological factors that contribute to the uncertainties in projecting cancer risks [1, 2] in future work.

1. INTRODUCTION

The risk of radiation-caused cancer and degenerative disease as well as acute radiation syndrome raises major concerns for astronauts' safety during space missions away from the protective zone of low-earth orbit [1, 2]. Solar particle events (SPEs) occur quite often and it is difficult to predict their onset and size. Most SPEs would result in small doses for the crew even with minimal spacecraft or spacesuit shielding, and only a small proportion (about 10%) of individual SPEs would be of concern to astronauts. However, the sum doses of many small events can disrupt mission operations and lead to excessive costs.

For longer duration space missions, chronic exposure to SPEs with intense particle fluxes and high energy levels is a major concern. However, the risk of early effects is expected to be small, due to the reduction of effects at the characteristic dose-rates of SPEs behind protective or tissue shielding (<0.3 Gy/h). However, a significant cancer risk does remain for some events [1-4]. As there are limitations in crew return vehicles, as well as the dose limits defined by NASA [5], accurate estimations of SPE frequencies and exposure levels during mission periods are necessary for protection of astronauts and for determining shielding requirements [4] for missions to the Moon and Mars. A probabilistic risk assessment approach is needed to implement the requirements for radiation protection from SPEs for astronauts and/or possible hardware failures.

Major SPEs were detected on Earth using a variety of measuring techniques during solar cycle 19, and since the solar cycle 20, SPEs have been routinely detected by satellites. The cumulative frequency curve was derived from the event-integrated fluences with energy above 30 MeV (Φ_{30}) without considering the event onset time. Using the 370 SPEs from all available recorded databases for solar cycles 19-23, we have developed a probabilistic modeling approach, where the best propensity for SPE occurrence as a function of time within a solar cycle was defined from a non-homogeneous Poisson model [6]. From the fitted model, the expected frequency of SPEs during a defined space mission period was estimated and its total proton fluence distribution of Φ_{30} was simulated with a random draw from a Gamma distribution for the given mission period.

For SPE risk analysis, analytic representations of energy spectra extending over broad energy ranges out to 1 GeV were fitted by Weibull-distributions to proton fluence measurements. The defined differential energy spectra

of SPEs are propagated through spacecraft and body tissue to a typical blood forming organ (BFO) site by using the Baryon transport code, BRYNTRN [7, 8]. The resultant BFO dose distribution from 34 historically large SPEs for an astronaut inside a moderately shielded spacecraft has been used for the analysis of BFO exposure level during a specific mission period. The risk assessment was made ranging from its 5th to 95th percentile with respect to the corresponding Φ_{30} fluence distribution. The probabilities of BFO doses exceeding the NASA recommended limit, which are functions of event size and shielding thickness, were calculated for various SPE intensities during transit to Moon/Mars and on lunar surface. The results provide useful guidelines for developing protection systems for astronauts during future space exploration missions.

Lifetime cancer mortality risk described as risk of exposure induced death (REID) is employed by NASA as the quantity for implementing the radiation protection principle of "As low as reasonably achievable", (ALARA). With the consideration of detailed shielding properties provided by a conceptual lunar habitat model, the probabilistic assessments of radiation cancer risk, which are dependent on age, gender, and solar modulation, were predicted at median and upper 95% confidence interval (CI) for various mission durations. Using the risk mitigation method for candidate spacecraft designs, the proper shielding requirements for crew members would be identified for future exploration mission scenarios.

2. DATABASE OF PROTON MEASUREMENTS OF SOLAR PARTICLE EVENTS

We considered all solar particle events (SPEs) for solar cycles 19-21 (1955-1986), and all available flux and fluence data assembled in the form of a continuous database [9-11]. From 1986 to 2007 (solar cycles 22 and 23), a SPE list and the Geostationary Operational Environmental Satellite (GOES) spacecraft measurements of the 5-min average integral proton flux were obtained through direct access to NOAA's National Geophysical Data Center (NGDC) [12]. For the completeness of the event-size of Φ_{30} for the past five solar cycles, the SPE fluences for solar cycles 19-21 were taken from the [9-11]. The fluences for cycles 22 and 23 were calculated using the extensive direct GOES satellite particle measurements of integral proton flux [12]. Between the years 1561 and 1950, 71 SPEs with Φ_{30}> 2×10^9 protons cm^{-2} [13, 14] were also identified from impulsive nitrate enhancements in polar ice cores. Tab. 1 lists all of the available data for SPEs for the omnidirectional proton fluence of Φ_E, where E=10, 30, 50, 60 or 100 MeV.

Table 1. Database of recorded SPEs

Solar Cycle	# of SPE	# of Day	Period	Φ_E
Cycle 23	92	4262	5/1/1996-12/31/2007*	$\Phi_{10,30,50,60,100}$ [12]
Cycle 22	77	3742	2/1/1986-4/30/1996	$\Phi_{10,30,50,60,100}$ [12]
Cycle 21	70	3653	2/1/1976-1/31/1986	$\Phi_{10,30}$ [9]
Cycle 20	63	4140	10/1/1964-1/31/1976	$\Phi_{10,30}$ [9] and $\Phi_{10,30,60}$ [10]
Cycle 19	68	3895	2/1/1954-9/30/1964	$\Phi_{10,30,100}$ [9] and $\Phi_{10,30}$ [11]
Impulsive Nitrate Events	71	390 years	1561-1950	Φ_{30} [13, 14]

*The end of Cycle 23 estimated

3. PREDICTION OF SPE FREQUENCY

The total of 370 SPEs identified during solar cycles 19–23 were statistically significantly different in the overall distribution of Φ_{30} from cycle to cycle. However, fluence data of Φ_{30} was combined over all 5 cycles to estimate an overall probability distribution of an average cycle. Fig. 1 shows sample cumulative tail probabilities of Φ_{30} for cycles 19-23 and the overall cumulative tail probability (thick line). Also included in Fig. 1 are the probabilities of the impulsive nitrate events of 71 SPEs with Φ_{30} > 2×10^9 protons cm^{-2} [13] with and without seasonal correction, and they are not significantly different from the modern sets of large Φ_{30} data [6].

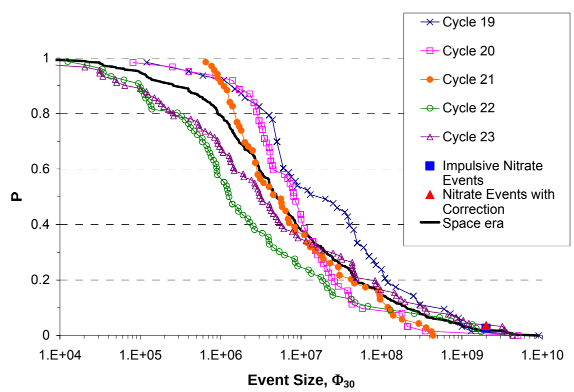

Figure 1. Probability (P) of an SPE event exceeding the displayed threshold Φ_{30}.

While the expected frequency of SPEs is strongly influenced by solar modulation, the SPE occurrences themselves are random in nature. The "spikes" in Fig. 2 show the onset times of all SPEs in solar cycles 19-23. Because there are typically more SPEs near the middle of cycles than near the beginning and end of cycles, the hazard function should take on relatively low values at

the ends of each solar cycle and reach a peak somewhere near the middle of cycles. After studying different models for the hazard function and assessing goodness of fit, the functional form best explaining all SPEs was found as in [6]

$$\lambda(t) = \frac{\lambda_0}{4000} + \frac{K}{4000}\frac{\Gamma(p+q)}{\Gamma(p)\Gamma(q)}\left(\frac{t}{4000}\right)^{p-1}\left(1-\frac{t}{4000}\right)^{q-1} \quad (1)$$

for a “typical” nonspecific cycle of 4000 days duration ($0 < t < 4000$), where λ_0, K, p, and q are parameters to be estimated. Resulting maximum-likelihood parameter estimates were $\lambda_0 = 19.52$, $K = 55.89$, $p = 4.073$ and $q = 4.820$. Also, from eqn (1), it can be shown that μ, the time of peak hazard, is $4000(p-1)/(p+q-2)$ days into a cycle. For the observed data, μ was estimated at 1783 days.

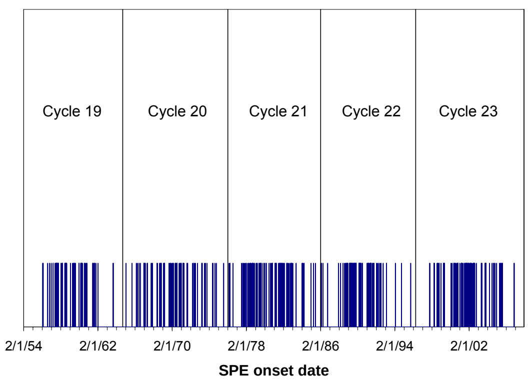

Figure 2. The onset dates of SPEs occurring between January 1, 1956 and December 31, 2007.

Using the basic properties of a Poisson process and the estimated $\lambda(t)$ at time t of a solar cycle, the expected number of events for a mission in a time interval (t_1, t_2), $N(t_1, t_2)$ were estimated more accurately than obtained by simple counting of cases in the SPE data occurred in a given time period (t_1, t_2). For conservatism, missions were assumed to take place centered on the time of greatest hazard, $\mu = 1783$ days into a solar cycle, so that $t_1 = 1783 - d/2$ and $t_2 = 1783 + d/2$, where d is mission length (days).

4. SIMULATION OF THE EVENT SIZE DISTRIBUTION

There isn’t any recognizable pattern of the event size distribution during the past 5 solar cycles and the event size Φ_{30} is independent of elapsed time between two consecutive events [6]. Therefore, the individual event size Φ_{30} for each SPE occurrence must be independent of the expected number of events for a given mission duration, $N(d)$. For the randomness of individual event size, its Φ_{30} was simulated with a random draw from a Gamma distribution. An empirical distribution of total fluence Φ_{30} ranging from the 5th to 95th percentile is shown in Fig. 3 for a range of potential mission lengths.

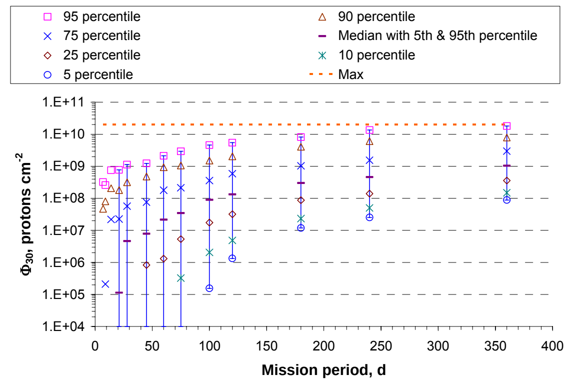

Figure 3. Simulated distribution of Φ_{30}.

5. CONTINUOUS ENERGY SPECTRUM OF SPE FOR RISK ANALYSIS

With the expected number of events, which took into account for the randomness of SPE occurrences, total event sizes of Φ_{30} in a mission period have been simulated ranging from its 5th to 95th percentile. The intense SPEs were considered as potentially debilitating events. In assessing radiation risk from SPEs during a given mission period, the simulation must take into account not only the randomness of SPE occurrences and event sizes of Φ_{30}, but also the variation of energy spectra for the SPEs, because the detailed SPE energy spectrum is the important parameter.

For the continuous fluence-energy spectrum of SPE, each SPE must be characterized from the individual measurements. Time-integrated integral proton fluence measurements of SPEs are available at discrete energies usually with >10, >30, >50, >60, or >100 MeV as listed in Tab. 1. Data at energies higher than 100 MeV are rather limited, and extrapolation to higher energies based on the spectral shape of individual SPE is necessary. A number of approaches to determine the spectral parameters have been reported [15-21]. Two fits, exponential rigidity and the Weibull distribution, are shown in Fig. 4 for the measurements of October 19, 1989 SPE, in which the measured spectrum extends to energies out to 100 MeV range. The continuous energy spectrum fitted by the Weibull parameterization shows to be accurate with the existing measurements of proton fluence at lower energies. Therefore, Weibull

distribution spectral parameters for 34 historically large SPEs in the space era [17] were used for the current risk assessments from SPEs.

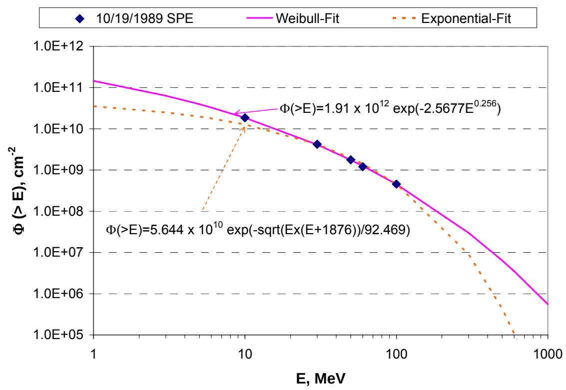

Figure 4. Fit to proton fluence measurements for continuous energy spectrum of October 19, 1989 SPE.

Radiation transport properties of shielding materials and the astronaut's body tissues were calculated using NASA's BRYNTRN code [7, 8]. The shielding distribution of the spacecraft was initially represented as a 5 g/cm^2-thick sphere of aluminum representing the equipment room of the vehicle. The body shielding distribution at the sensitive organ sites was obtained using the computerized anatomical man (CAM) model [22]. The resultant blood forming organ (BFO) doses from 34 large SPEs are shown in Fig. 5 (filled square). The solid line is the linear regression fit of BFO dose as a function of event size of Φ_{30} on a log-log scale. A SPE above the regression line is considered to be a "hard" spectrum (e.g., July 1961 SPE), on or very near the line as "median" spectrum (e.g., August 1972 SPE, October 1992 SPE, and April 2002 SPE), and below the line as a "soft" spectrum for any event of fluence Φ_{30}. For each event and corresponding fluence in Fig. 5, the BFO dose distribution is simulated by a random draw from a normal distribution about the regression line, which is attributable to the variability of SPE spectra. The vertical lines in Fig. 5 represent a range from the 5th to the 95th percentile of the distribution of the BFO dose, which results from the variability of the SPE spectra of the same event size Φ_{30}. Also, included in Fig. 5 as a horizontal dashed line is the current NASA 30-day BFO dose limit [23] of 25 cGy-Eq. Using this fitted regression model, the probability of exceeding the NASA 30-day limit dose was calculated as a function of Φ_{30} for an aluminum vehicle with 5 or 10 g/cm^2-thickness located in interplanetary space or on the lunar surface. These are shown in Fig. 6.

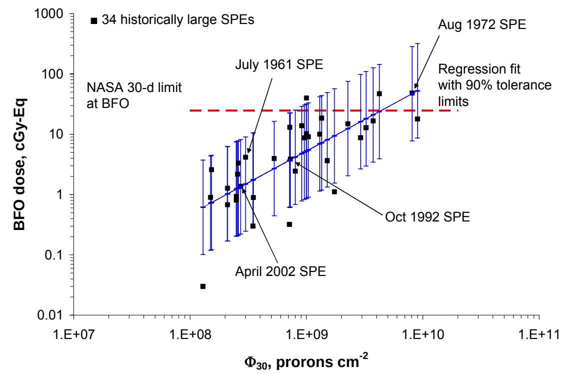

Figure 5. BFO dose of 34 large SPEs inside an equipment room in interplanetary space.

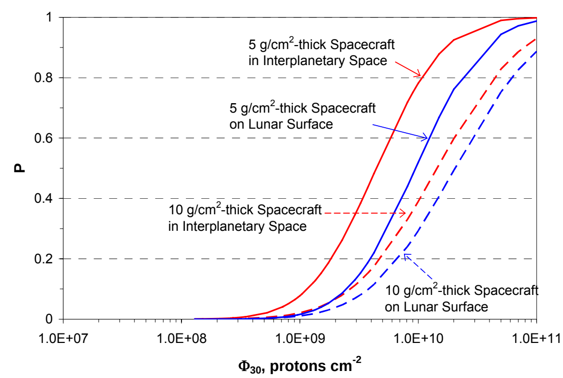

Figure 6. Probability of exceeding the NASA 30-d limit of BFO dose as a function of Φ_{30}, shield, and location.

6. ORGAN DOSE AND PROBABILISTIC ASSESSMENT OF CANCER RISK WITH CONCEPTUAL LUNAR HABITAT

Organ dose calculations were made with the CAM model [22], which represents the self-shielding of the human body in a water equivalent mass approximation. The whole body effective dose is defined as a summation over radiation types and organ/tissues using the tissue weighting factors, w_T [24].

The amount of directional shielding offered by all of the structural components and contents of the vehicle, such as various racks, equipment, and inner and outer shell materials of a conceptual lunar habitat design[1], was accounted for in the radiation risk assessment at specific positions of the storm shelter and living area. The storm shelter was located in the sleep area, in which 10 g/cm^2 of water wall shields were added to the outer upper wall and the side upper wall. It added a total of 623 kg of

[1] Credit to G. Qualls at NASA Langley Research Center for ray tracing of conceptual lunar habitat design.

water weight to the habitat. The event-specific whole body effective doses are presented in Tab. 2 for the storm shelter and living area inside the lunar habitat for various SPE spectra, including the Weibull distribution of the July 1961 SPE hard spectrum, three other Weibull distributions as median spectra, and the King spectrum of August 1972 SPE as a design standard recommended in [23].

Table 2. Whole body effective dose from each SPE at two positions inside a conceptual lunar habitat.

SPE	Weibull Distribution				
	Φ_{30}, p/cm^{-2}	Effective dose, mSv			
		Strom shelter		Living area	
		Male	Female	Male	Female
7/18/1961	$3x10^8$	9.2	9.3	17.5	17.5
4/21/2002	$2.72x10^8$	1.9	1.9	6.7	6.4
10/30/1992	$7.27x10^8$	6.8	6.8	17.9	17.3
8/2/1972	$8.1x10^9$	67.6	66.9	234.1	221.7
Aug 1972 King Spec	$8.1x10^9$	58.88	57.4	234.7	219.6

Whole body effective doses for the given mission periods were calculated by scaling the SPE fluence with its specific spectral variation to the total SPE fluences of Φ_{30} at median and upper 95% confidential interval for 90 and 365 day lunar missions (Tab. 3 and 4, respectively). From these results, the King Spectrum of the August 1972 SPE is recognized as a design standard for the cancer risk assessment in this study, because it reasonably represents SPE spectral variability of the median level events.

Table 3. Whole body effective dose from total SPE fluence for 90-d lunar mission

(a) SPE at Median

SPE	Φ_{30}	Scale	Effective dose at Median SPE for 90-d, mSv			
			Strom shelter		Living area	
			M	F	M	F
7/18/1961	$6.2x10^7$	0.21	1.90	1.92	3.62	3.62
4/21/2002	$6.2x10^7$	0.23	0.43	0.43	1.53	1.46
10/30/1992	$6.2x10^7$	0.09	0.58	0.58	1.53	1.48
8/2/1972	$6.2x10^7$	0.01	0.52	0.51	1.79	1.70
Aug 1972 King Spec	$6.2x10^7$	0.01	0.45	0.44	1.80	1.68

(b) SPE at upper 95% CI

SPE	Φ_{30}	Scale	Effective dose at Upper 95% CI SPE for 90-d, mSv			
			Strom shelter		Living area	
			M	F	M	F
7/18/1961	$1.0x10^{10}$	33.33	307	310	583	583
4/21/2002	$1.0x10^{10}$	36.76	70	70	246	235
10/30/1992	$1.0x10^{10}$	13.76	94	94	246	238
8/2/1972	$1.0x10^{10}$	1.23	84	83	289	274
Aug 1972 King Spec	$1.0x10^{10}$	1.23	73	71	290	271

Table 4. Whole body effective dose from total SPE fluence for 365-d lunar mission.

(a) SPE at Median

SPE	Φ_{30}	Scale	Effective dose at Median SPE for 365-d, mSv			
			Strom shelter		Living area	
			M	F	M	F
7/18/1961	$1.06x10^9$	3.53	32.5	32.9	61.8	61.8
4/21/2002	$1.06x10^9$	3.90	7.4	7.4	26.1	24.9
10/30/1992	$1.06x10^9$	1.46	9.9	9.9	26.1	25.2
8/2/1972	$1.06x10^9$	0.13	8.9	8.8	30.6	29.0
Aug 1972 King Spec	$1.06x10^9$	0.13	7.7	7.5	30.7	28.7

(b) SPE at Upper 95% CI

SPE	Φ_{30}	Scale	Effective dose at Upper 95% CI SPE for 365-d, mSv			
			Strom shelter		Living area	
			M	F	M	F
7/18/1961	$1.89x10^{10}$	63.00	580	586	1103	1103
4/21/2002	$1.89x10^{10}$	69.49	132	132	466	445
10/30/1992	$1.89x10^{10}$	26.00	177	177	466	450
8/2/1972	$1.89x10^{10}$	2.33	158	156	546	517
Aug 1972 King Spec	$1.89x10^{10}$	2.33	137	134	548	512

Career exposure to radiation is limited by NASA so as not to exceed 3% risk of exposure induced death (REID) from fatal cancer. NASA policy is to assure that this risk limit is not exceeded at the 95% confidence level, using a statistical assessment of the uncertainties in the risk projection calculations to limit the cumulative effective dose (in units of Sievert) received by an astronaut throughout his or her career. These limits are applicable to missions in low Earth orbit (LEO) of any duration, and to lunar missions of less than a certain number of days. Non-cancer mortality risks and approaches to reducing uncertainties in cancer risk projection models must be considered further for longer missions outside LEO.

The relationship between radiation exposure and risk is both age and gender specific, due to latency effects, and to differences in tissue types, sensitivities, and life-span expectations. These relationships are estimated using the methods recommended by the NCRP [5], and more recent radiation epidemiology research [26, 27]. The cancer fatality risk (%REID) to an astronaut during a

space mission is found by applying the double-detriment life table using the tissue-weighted effective dose, *E*, and time-dependent relative risk functions [4].

The current NASA model [5] was based on life-span studies (LSS) of atomic bomb survivors, since the doses received by the LSS population overlap strongly with the doses of concern to NASA exploration missions [26]. The most recent and extensive review of data sets from human populations, including nuclear reactor workers and patients treated with radiation, was reported in Biological Effects of Ionizing Radiation (BEIR) VII [27]. Cancer fatality risk of %REID as functions of age at exposure, gender, and solar cycle dependence was calculated using two projection models for various lunar mission periods: in Tab. 5a for the missions at solar maximum, and in Tab. 5b for those at solar minimum.

Table 5a. Cancer fatality risk of %REID at solar maximum

		90-d mission				180-d mission				365-d mission			
		Male		Female		Male		Female		Male		Female	
Effective dose at median, mSv		35.4		35.7		72.1		72.6		149.4		150.3	
Effective dose at upper 95% CI		107.6		106.1		157.1		155.5		279.1		276.7	
%REID Carcino-genesis	Age, yr	NASA Model	BEIR-VII	NASA Model	BEIR-VII	NASA Model	BEIR-VII	NASA Model	BEIR-VII	NASA Model	BEIR-VII	NASA Model	BEIR-VII
Median	35	0.14	0.14	0.17	0.19	0.28	0.27	0.35	0.38	0.57	0.56	0.71	0.78
	40	0.12	0.13	0.15	0.19	0.25	0.27	0.31	0.38	0.52	0.55	0.63	0.77
	45	0.11	0.13	0.13	0.18	0.22	0.26	0.26	0.37	0.45	0.53	0.54	0.75
	50	0.09	0.12	0.11	0.17	0.19	0.25	0.22	0.36	0.38	0.51	0.46	0.72
	55	0.08	0.12	0.09	0.16	0.16	0.24	0.19	0.33	0.33	0.48	0.38	0.68
Upper 95% CI	35	1.1	1.1	1.3	1.5	1.7	1.7	2.1	2.3	3.2	3.1	3.9	4.2
	40	1.0	1.1	1.2	1.5	1.6	1.7	1.9	2.3	2.8	3.0	3.4	4.2
	45	0.9	1.0	1.0	1.4	1.3	1.6	1.6	2.2	2.5	2.9	2.9	4.1
	50	0.7	1.0	0.9	1.4	1.2	1.5	1.4	2.2	2.1	2.8	2.5	3.9
	55	0.6	0.9	0.7	1.3	1.0	1.5	1.2	2.0	1.8	2.6	2.1	3.7

Table 5b. Cancer fatality risk of %REID at solar minimum

		90-d mission				180-d mission				365-d mission			
		Male		Female		Male		Female		Male		Female	
Effective dose, mSv		76		76		152		152		304		305	
%REID Carcino-genesis	Age, yr	NASA Model	BEIR-VII	NASA Model	BEIR-VII	NASA Model	BEIR-VII	NASA Model	BEIR-VII	NASA Model	BEIR-VII	NASA Model	BEIR-VII
Median	35	0.29	0.28	0.29	0.4	0.58	0.57	0.72	0.79	1.16	1.13	1.44	1.58
	40	0.26	0.28	0.26	0.39	0.52	0.56	0.64	0.78	1.04	1.11	1.27	1.56
	45	0.23	0.27	0.23	0.38	0.45	0.54	0.54	0.76	0.90	1.08	1.08	1.52
	50	0.19	0.26	0.19	0.37	0.39	0.52	0.46	0.73	0.78	1.04	0.92	1.46
	55	0.17	0.25	0.17	0.35	0.33	0.49	0.39	0.69	0.66	0.98	0.77	1.37
Upper 95% CI	35	1.1	1.1	1.1	1.6	2.3	2.3	2.8	3.1	4.6	4.5	5.7	6.2
	40	1.0	1.1	1.0	1.5	2.1	2.2	2.5	3.1	4.1	4.4	5	6.2
	45	0.9	1.1	0.9	1.5	1.8	2.1	2.1	3.0	3.6	4.3	4.3	6.0
	50	0.8	1.0	0.8	1.5	1.5	2.1	1.8	2.9	3.1	4.1	3.6	5.8
	55	0.7	1.0	0.7	1.4	1.3	1.9	1.5	2.7	2.6	3.9	3.0	5.4

7. CONCLUSION

For managing space radiation risk in the new era of space exploration, the sporadic distribution of SPE occurrences in a given mission period was analyzed by employing a probabilistic approach using data from all the recorded SPEs. This model-based estimate has shown to be considerably more accurate than one based on simple counting of historical events, of which there may be very few within the time window. Next, the distribution of total fluences of SPEs in a given mission period was simulated by a random draw from Gamma distribution due to the randomness of individual event size. The exposure risk from each event with its corresponding fluence is distributed as a normal distribution about the regression line, which is attributable to the variability of detailed SPE spectra, by which probability of exceeding the current NASA limit

can be calculated for the guidelines in developing spacecraft design. In assessing radiation risk from SPEs for a range of potential mission lengths, the simulation took into account not only the randomness of SPE occurrences and individual event sizes, but also the variability of SPE energy spectra. Based on the probabilistic assessment of radiation risk of a conceptual lunar habitat model, lunar missions up to 210-day are allowed at solar maximum, but those to 90-day are allowed at solar minimum, because the fatal cancer risks for astronauts during those mission periods are within the maximum acceptable levels of 3% at the upper 95% confidence interval. The results will be useful in developing guidelines for protection systems for astronauts during future space exploration missions.

8. REFERENCES

1. Cucinotta, F.A., Schimmerling, W., Wilson, J.W., Peterson, L.E., Saganti, P., Badhwar, G.D. & Dicello, J.F. (2001). Space Radiation Cancer Risks and Uncertainties for Mars Missions. *Radiat Res* **156**, 682-688.
2. Cucinotta, F.A. & Durante. M. (2006). Cancer Risk from Exposure to Galactic Cosmic Rays: Implications for Space Exploration by Human Beings. *Lancet Oncol* **7,** 431-435.
3. Cucinotta, F.A. (1999). Issues in risk assessment from solar particle events. *Radiat Meas* **30**, 261-268.
4. Cucinotta, F.A., Kim, M.H. & Ren. L. (2006). Evaluating Shielding Effectiveness for Reducing Space Radiation Cancer Risks. *Radiat Meas* **41**(9-10), 1173-85.
5. National Council on Radiation Protection and Measurements (NCRP) 2000. *Radiation protection guidance for activities in low-Earth orbit*. Bethesda, Maryland: National Council on Radiation Protection and Measurements; NCRP Report No. 132.
6. Kim, M.Y., Hayat, M.J., Feiveson, A.H. & Cucinotta, F.A. (submitted). Prediction of Frequency and Exposure Level of Solar Particle Events, *Health Physics*.
7. Wilson, J.W., Townsend, L.W., Nealy, J.E., Chun, S.Y., Hong, B.S., Buck, W.W., Lamkin, S.L., Ganapole, B.D., Kahn, F. & Cucinotta, F.A. (1989). *BRYNTRN: A Baryon transport model*. Washington DC: NASA; Report No. TP-2887.
8. Cucinotta, F.A., Wilson, J.W. & Badavi, F.F. (1994). *Extension to the BRYNTRN code to monoenergetic light ion beams*. Washington DC, NASA Report No. TP-3472.
9. Feynman, J., Armstrong, T.P., Dao-Gibner, L. & Silverman, S. (1990). *J. Spacecraft*, **27(**4), 403-410.
10. King, J.H. (1974). Solar Proton Fluences for 1977-1983 Space Missions, *J. Spacecraft*, **11**(6), 401-408.
11. Shea, M. & Smart, D. (1990). *Solar Physics*, **127**, 297-320.
12. GOES SEM data: http://goes.ngdc.noaa.gov/data/
13. McCracken, K.G., Dreschhoff, G.A.M., Zeller, E.J., Smart, D.F. & Shea, M. A. (2001). Solar Cosmic Ray Events for the Period 1561-1994, 1. Identification in Polar Ice, 1561-1950. *J. Geophys. Res*., **106**(A10), 21585-21598.
14. Siverman, S.M. (2005). The earliest recorded aurora in North America since European colonization, *J. Atmospheric and Solar-Terrestrial Physics*, 67(7)**,** 749-752.
15. Freier, P.S. & Webber, W.R. (1963). Exponential Rigidity Spectrums for Solar-Flare Cosmic Rays, *J. Geophys. Res*., **68**(6), 1605-1629.
16. Biswas S., Fichtel, C.E. & Guss, D.E. (1962). Study of the Hydrogen, Helium, and Heavy Nuclei in the November 12, 1960 Solar Cosmic-Ray Event. *Phys. Review*, **128**(6), 2756-2771.
17. Kim, M.Y., Cucinotta, F.A. & Wilson, J.W. (2007). A Temporal Forecast of Radiation Environments for Future Space Exploration Missions. *Radiat. and Environ. Biophys*., **46**(2), 95-100.
18. Kim, M.Y., Cucinotta, F.A. & Wilson, J.W. (2006). Mean Occurrence Frequency and Temporal Risk Analysis of Solar Particle Events, *Radiat. Meas.*, **41**, 1115-1122.
19. Xapsos, M. *et al*. (2000). *IEEE Trans. Nuc. Sci.* **47**(6), 2218-2223.
20. Kim, M.Y., Wilson, J.W., Cucinotta, F.A., Simonsen, L.C., Atwell, W., Badavi, F.F. & Miller, J. (1999). *Contribution of HZE Ions During the September 29, 1989 Solar Particle Event*, NASA-TP-1999-209320.
21. Nymmik R.A. (1999). Probabilistic model for fluences and peak fluxes of solar energetic particles. *Radiat Meas* 30, 287-296.
22. Billings M.P. & Yucker W.R. (1973). *The computerized anatomical man (CAM) model*. Washington DC, NASA CR-134043.
23. National Research Council/National Academy of Sciences (NRC/NAS). (2008). Committee on the Evaluation of Radiation Shielding for Space Exploration. *Managing space radiation risk in the new era of space exploration*. National Academies

Press. [ISBN: 0-309-11383-0].

24. ICRP Publication 103. (2008). *Recommendations of the International Commission on Radiological Protection*. Annals of the ICRP, **37**(2-4).

25. Preston, D.L., Shimizu, Y., Pierce, D.A. *et al.* (2003). Studies of Mortality of Atomic Bomb Survivors. Report 13: Solid Cancer and Noncancer Disease Mortality: 1950–1997. *Radiat Res* **160**, 381–407.

26. Cucinotta, F.A., Kim, M.Y. & Ren, L. (2005). *Managing Lunar and Mars Mission Radiation Risks, Part I: Cancer Risks, Uncertainties, and Shielding Effectiveness*, Washington DC, NASA TP 2005-213164.

27. National Research Council/National Academy of Sciences (NRC/NAS). (2006). Committee to Assess Health Risks from Exposure to Low Levels of Ionizing Radiation, *Health Risks from Exposure to Low Levels of Ionizing Radiation: BEIR VII*. National Academies Press. [ISBN: 0-309-09156-X].